

Adaptive Modulation Using Outdated Samples of Another Fading Channel

Tung-Sheng Yang and Alexandra Duel-Hallen
North Carolina State University
Dept. of Electrical and Computer Engineering
Center for Advanced Computing and Communication
Box 7914, Raleigh NC 27695-7914

Abstract—Adaptive transmission techniques, such as adaptive modulation and coding, adaptive power control, adaptive transmitter antenna diversity, etc., generally require precise channel estimation and channel state information (CSI) feedback. For fast vehicle speeds, reliable adaptive transmission also requires prediction of future CSI since the channel conditions are rapidly time-variant. In this paper, we propose to use past channel observations of one carrier to predict future CSI and perform adaptive modulation without feedback for another correlated carrier. Statistical model of the prediction error that depends on the frequency and time correlation is developed and is used in the design of reliable adaptive modulation methods. Significant gains relative to non-adaptive techniques are demonstrated for sufficiently correlated channels and realistic prediction range.

1. INTRODUCTION

High-speed wireless communications require robust channel estimation and adaptive transmission to satisfy the tremendous growth in demand for capacity. The idea of adaptive transmission [1-4] is to change the transmission parameters according to the instantaneous fading channel power without sacrificing bit-error rate (BER). In particular, adaptive modulation can provide higher bit rates relative to conventional signaling by transmitting at high rate under favorable channel conditions, and reducing throughput as the channel degrades. Adaptive modulation depends on accurate CSI that can be acquired from different sources. If the communication between the two stations is bi-directional and the channel can be considered reciprocal, then each station can estimate the channel quality on the basis of the received symbols and adapt the parameters to this estimation. This is called open-loop adaptation [5]. If the channel is not reciprocal, the receiver has to estimate the channel quality from feedback resulting in closed-loop adaptation. The feedback delay, overhead, and processing delay will degrade the system performance of the adaptive modulation, especially in rapidly time variant fading. Even in open-loop channels, current CSI is not sufficient since future channel conditions need to be known to adapt transmission parameters. To realize the potential of adaptive transmission methods, the channel variations have to be reliably predicted at least several milliseconds ahead.

Recently, a novel adaptive long-range prediction method was proposed in [6-11]. The algorithm employs an autoregressive (AR) model to characterize the fading channel and computes the minimum mean-square-error (MMSE) estimate of a future fading coefficient based on a number of past observations. The advantage of this algorithm relative to

conventional methods is due to its low sampling rate (on the order of twice the maximum Doppler shift and much lower than the data rate), which results in longer memory span for a fixed filter length. This allows to sample large sidelobes of the autocorrelation function of the Rayleigh fading channel, and thus to predict further into the future.

In this paper, we extend the long-range prediction algorithm into frequency domain. In particular, we concentrate on the scenario where received uplink signal is observed at the carrier frequency f^1 and adaptive transmission is performed in the downlink signal at the carrier frequency f^2 without feedback from the mobile. Alternatively, a signal at frequency f^1 can be fed back and used to select parameters for adaptive signaling at adjacent frequency f^2 . To accomplish this adaptive transmission reliably, the transmitted signal must be sufficiently correlated with the observation in both time and frequency. This technique can be applied in correlated uplink and downlink channels, in orthogonal frequency division multiplexing (OFDM) systems (where narrow correlated sub-channels are employed) or other wideband systems to reduce feedback and overhead requirements.

The remainder of this paper is organized as follows. In the next section, we present the system model and describe the long-range prediction technique, the statistical model of the prediction error and channel statistics. In section 3, the adaptive modulation scheme is discussed and the performance of adaptive modulation aided by the proposed long-range prediction method is demonstrated.

2. SYSTEM MODEL AND PREDICTION METHOD

The discrete-time system model is illustrated in Fig. 1. The carrier frequency of observed CSI is f^1 and the carrier frequency of the transmitted signal is f^2 . The statistics of fading signals received at correlated carriers are discussed in [12]. The fading coefficients at two frequencies can be expressed as:

$$c(f^1, t) = \sum_{n=1}^N A_n e^{j(2\pi f_n t + \phi_{1n})} \quad (1)$$

$$c(f^2, t) = \sum_{n=1}^N A_n e^{j(2\pi f_n t + \phi_{2n})}$$

where for the n^{th} path, A_n is the (real) amplitude and f_n is the Doppler shift. The phase difference of the n^{th} path $\phi_{2n} - \phi_{1n} = 2\pi \Delta f T_n$ where $\Delta f = f_2 - f_1$ is the frequency separation, and T_n is the delay spread. For large N , $c(f^n, t)$ is

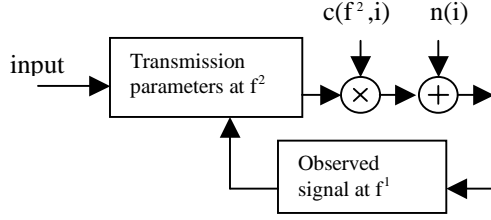


Fig. 1. System model

distributed approximately as a zero mean complex Gaussian random variable. Hence the amplitudes $\alpha(f^1, t) = |c(f^1, t)|$ and $\alpha(f^2, t) = |c(f^2, t)|$ are both Rayleigh distributed. Assume angular distribution of the incident power is uniform between $[0, 2\pi]$, horizontal directivity pattern of the receiving antenna is 1, and the delay spread T_n is exponentially distributed [12] with the probability density function (pdf):

$$p(T) = \frac{1}{\sigma} e^{-T/\sigma} \quad (2)$$

where σ is a measure (rms delay spread [14]) of the time delay spread. The cross-correlation of the two fading signals with the time difference $\tau = |t_1 - t_2|$ and the frequency separation $\Delta f = f^2 - f^1$ can be derived as:

$$R(\tau, \Delta f) = E[c(f^1, t) c^*(f^2, t + \tau)] = R_c(\tau) R_f(\Delta f) \quad (3)$$

where $R_c(\tau) = J_0(2\pi f_{dm} \tau)$ is the zero order Bessel function and

$$R_f(\Delta f) = \frac{1}{1 + (2\pi \Delta f \sigma)^2} - j \frac{2\pi \Delta f \sigma}{1 + (2\pi \Delta f \sigma)^2} \quad (4)$$

Define $\Delta f \sigma$ as the normalized frequency separation. The cross-correlation (3) vs. $\Delta f \sigma$ for $\tau = 0$ is plotted in Fig. 2. We also plotted the numerical cross-correlation of generated fading signals for comparison. To generate the signals, $c(f^1, t)$ was created first using Jakes model [12]. In this paper, we employ the 9 oscillators Jakes model with the maximum Doppler shift $f_{dm} = 100\text{Hz}$. Then $c(f^2, t)$ was generated from $c(f^1, t)$ using the same parameters except phases $\phi_{2n} = \phi_{1n} + 2\pi \Delta f T_n$. Multiple experiments were performed using independent realization of delay spreads T_n according to (2) and the ensemble average of cross-correlation was computed. Using this fading model, we characterize the capability of the proposed method to enable adaptive modulation.

Let $c(f^n, i)$, $n = 1, 2$, be samples of the fading signal $c(f^n, t)$ (1) at the sampling interval T_s . We assume that $E[|c(f^n, i)|^2] = 1$. The linear MMSE prediction of the future channel sample $c(f^2, n)$ at frequency f^2 based on p previously observed samples $c(f^1, n-j)$ at frequency f^1 is given by:

$$\hat{c}(f^2, n) = \sum_{j=1}^p d_j c(f^1, n-j) \quad (5)$$

The optimal coefficients d_j are determined as:

$$\underline{d} = \underline{R}^{-1} \underline{r} \quad (6)$$

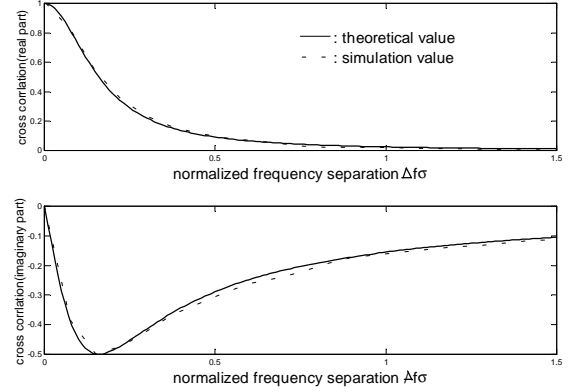


Fig. 2. Cross-correlation vs. normalized frequency separation $\Delta f \sigma$ for $\tau = 0$

where $\underline{d} = (d_1 \dots d_p)^T$, \underline{R} is the autocorrelation matrix ($p \times p$) with coefficients $R_{ij} = E[c(f^1, n-j) c^*(f^1, n-i)]$ and \underline{r} is the autocorrelation vector ($p \times 1$) with coefficients $r_j = E[c(f^2, n) c^*(f^1, n-j)]$. The resulting MMSE is given by:

$$E[|e(n)|^2] = E[|c(f^2, n) - \hat{c}(f^2, n)|^2] = 1 - \sum_{j=1}^p d_j^* r_j \quad (7)$$

In practice, the samples $c(f^1, n)$ are observed in the presence of complex additive white Gaussian noise (AWGN) $n(i)$ with power spectrum density (PSD) N_0 . Equations (5-7) can be easily modified to include noisy observations similarly to the derivation in [7]. Moreover, the effect of noise can be significantly reduced when prediction is combined with adaptive tracking [7,10]. In the prediction techniques employed in this paper, we use noiseless observation, the model order $p = 100$, the sampling rate is 500Hz and the observation interval is 100 samples. All results are obtained for the maximum Doppler shift of 100Hz.

If the channel statistics, such as the time and frequency domain correlation, are known, the optimum MMSE channel prediction can be employed as in (5-6). However, as the Doppler shifts in (1) vary, the model coefficients need to be updated continuously based on the observations. Since we are not able to observe the fading coefficients at frequency f^2 , we modify our approach as follows. The basic idea is to predict future channel coefficient $c(f^1, t)$ first and then to use the frequency correlation function to select the transmitter parameters at f^2 . The predicted CSI at f^1 are given by:

$$\hat{c}(f^1, n) = \sum_{j=1}^p g_j c(f^1, n-j) \quad (8)$$

The coefficients g_j are determined using the Least Mean Square (LMS) adaptive tracking method:

$$g_j(n) = g_j(n-1) + \mu \epsilon_n^* c(f^1, n-j) \quad (9)$$

where μ is the step size and $\epsilon_n = c(f^1, n) - \hat{c}(f^1, n)$. This adaptive tracking can be performed since the observations at

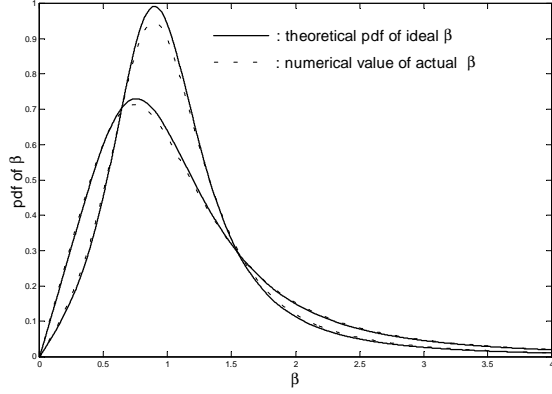


Fig. 3. PDF of ideal and actual accuracy factor β obtained using prediction at f^1 . $f_{dm}=100\text{Hz}$ and $\tau=2\text{ms}$.

frequency f^1 are available at the transmitter [7,8,10]. Recursive least square (RLS) can also be used to improve accuracy and reduce the observation interval [15].

Once $\hat{c}(f^1, n)$ is found, the adaptive modulation parameters for transmitting at f^2 at time n are selected as explained in section 3. Note that $\hat{c}(f^2, n)$ is not predicted directly. Instead, the prediction at frequency f^1 at time t serves as an estimate of $c(f^2, t)$. Suppose $\alpha = \alpha(f^2, t)$ is the actual fading amplitude and $\hat{\alpha} = |\hat{c}(f^1, n)|$ is its estimate. From [9], the prediction accuracy factor $\beta = \alpha/\hat{\alpha}$ has the pdf:

$$p_{\beta}(x) = \frac{2x(\frac{1}{\lambda}x^2 + \lambda)(1-\rho)}{((\frac{1}{\lambda}x^2 + \lambda)^2 - 4\rho x^2)^{1.5}} \quad (10)$$

where the correlation coefficient $\rho = \frac{\text{Cov}(\alpha^2, \hat{\alpha}^2)}{\sqrt{\text{Var}(\alpha^2)\text{Var}(\hat{\alpha}^2)}}$, and

$\lambda = \sqrt{\Omega/\hat{\Omega}}$, where $\Omega = E\{\alpha^2\}$ and $\hat{\Omega} = E\{\hat{\alpha}^2\}$. In Fig. 3, we compare the ideal $\beta = \frac{\alpha(f^2, t)}{\alpha(f^1, t)}$ obtained assuming perfect prediction at frequency f^1 , and actual accuracy factor obtained using predicted CSI at f^1 (prediction range is 2 ms (one step ahead)) for $f_{dm}=100\text{Hz}$. Two different values of normalized frequency separation are used. The pdf of ideal β is given by (10) with $\lambda = 1$ and $\rho = 1/(1+(2\pi\Delta f\sigma)^2)$. The actual pdf of β is obtained by numerical estimation of ρ and λ in (10).

3. ADAPTIVE TRANSMISSION USING LONG RANGE CHANNEL PREDICTION

In this paper, we employ variable rate and variable power square M-QAM signal constellations due to their inherent spectral efficiency and ease of implementation [13]. Given fixed transmitter power per symbol E_s (or average SNR level $\bar{\gamma} = E_s/N_0$) and a target bit error rate BER_{ig} , we adjust the modulation level M according to the instantaneous predicted

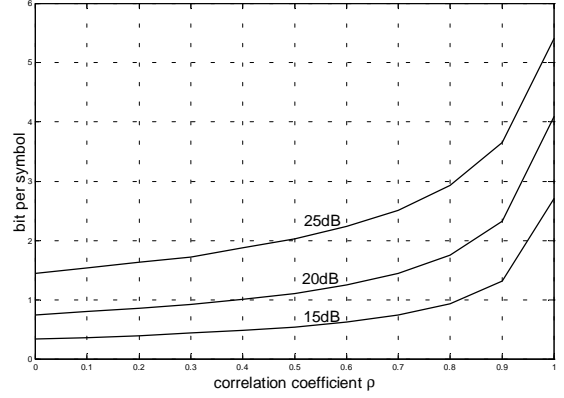


Fig.4. Bit per symbol vs. ρ for different SNR for power control M-QAM. Target $\text{BER}=10^{-3}$. $\lambda = 1$.

channel gain $\hat{\alpha}(i)$ using the distribution of the predicted accuracy factor β . Assume $\hat{\alpha}$ is the predicted channel gain $\hat{\alpha}(f^2, t)$ and $p_{\beta}(x)$ is given by (10). Throughout the paper, we employ an adaptive modulation scheme with the thresholds α_i , $i=1\dots 4$ chosen as follows. When the predicted channel gain $\hat{\alpha}$ satisfies $\alpha_{i+1} \geq \hat{\alpha} \geq \alpha_i$, $M(i)$ -QAM is employed, where $M(1)=2, M(i)=2^{2(i-1)}$, $i=2\dots 4$, ($\alpha_5 = \infty$) based on:

$$\text{BER}_{M(i)}^*(\bar{\gamma}, \hat{\alpha}) = \int_0^{\infty} \text{BER}_{M(i)}(\bar{\gamma}x^2\hat{\alpha}^2)p_{\beta}(x) dx \leq \text{BER}_{ig} \quad (11)$$

where $p_{\beta}(x)$ is described by (10). The $\text{BER}_{M(i)}$ is calculated from the BER bound of MQAM for an AWGN channel [1]:

$$\begin{aligned} \text{BER}_{M(i)}(\gamma) &\leq 0.2\exp(-1.5\gamma/(M(i)-1)) \quad M(i) \geq 4 \\ \text{BER}_{M(1)}(\gamma) &= Q(\sqrt{2\gamma}) \end{aligned} \quad (12)$$

where γ is the signal-to-noise ratio per symbol.

The BER of this fixed power discrete rate adaptive modulation is lower than the BER_{ig} since the thresholds α_i are chosen using the upper bound in (11). Below we describe a power control policy that maintains the target BER. From (11), when input power E_s is multiplied by $(\alpha_i/\hat{\alpha})^2$, the $\text{BER}_{M(i)}^*(\bar{\gamma}, \hat{\alpha})$ becomes:

$$\text{BER}_{M(i)}^*(\bar{\gamma}, \hat{\alpha}) = \int_0^{\infty} \text{BER}_{M(i)}(\bar{\gamma}x^2\alpha_i^2)p_{\beta}(x) dx = \text{BER}_{ig} \quad (13)$$

Another discrete rate variable power adaptive transmission scheme was proposed in [1]. The simpler method described above results in less than 0.5dB power loss compared to [1]. The proposed power control method can be simplified further by updating transmitted power at the low sampling rate (using predicted $\hat{\alpha}_n$) rather than employing interpolated $\hat{\alpha}$ and varying power at the symbol rate. Furthermore, a constant power level can be selected for each constellation M_i using:

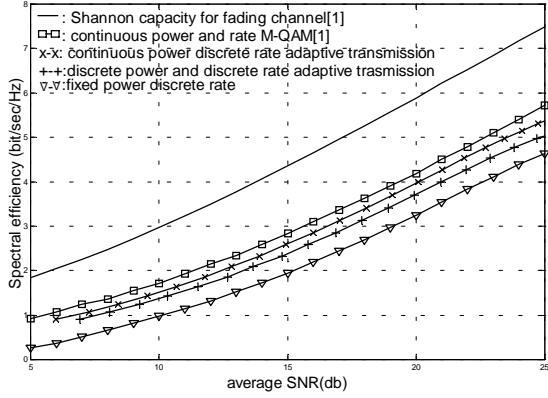


Fig. 5. Spectral efficiency vs. SNR for different transmission techniques. Target BER = 10^{-3} .

$$\int_{\alpha_i}^{\alpha_{i+1}} \text{BER}_{M(i)} \left(\frac{E_s(i)}{N_0}, \hat{\alpha} \right) p(\hat{\alpha} | \alpha_i < \hat{\alpha} < \alpha_{i+1}) d\hat{\alpha} \leq \text{BER}_{\text{tg}} \quad (14)$$

where $\text{BER}_{M(i)} \left(\frac{E_s(i)}{N_0}, \hat{\alpha} \right)$ is computed in (11) and $p(\hat{\alpha} | \alpha_i < \hat{\alpha} < \alpha_{i+1})$ is the conditional pdf of $\hat{\alpha}$ determined using thresholds α_i also chosen using (11). This method is called discrete rate discrete power [1].

The average bit rate per symbol \hat{R}_{ada} of adaptive modulation methods is defined as:

$$\hat{R}_{\text{ada}} = \sum_{i=1}^4 \log_2 M_i \int_{\alpha_i}^{\alpha_{i+1}} p_{\hat{\alpha}}(x) dx \quad (15)$$

This rate also gives the spectral efficiency assuming the ideal Nyquist data pulse. For the power control method above, the average transmission power P_{avg} is

$$P_{\text{avg}} = \sum_{i=1}^4 \int_{\alpha_i}^{\alpha_{i+1}} E_s \left(\frac{\alpha_i}{\alpha} \right)^2 p_{\hat{\alpha}}(x) dx \quad (16)$$

where the pdf of predicted amplitude $p_{\hat{\alpha}}(x)$ is:

$$p_{\hat{\alpha}}(x) = \frac{2x}{\Omega} \exp\left(-\frac{x^2}{\Omega}\right) \quad (17)$$

We plot the BPS (15) vs. the correlation ρ in (10) for this method for different SNR computed from (16) with $\lambda = 1$ and $\text{BER}_{\text{tg}} = 10^{-3}$ in Fig.4. The correlation $\rho = 1$ corresponds to perfect prediction, while $\rho = 0$ represents the worst case when the BPS of the adaptive modulation converges to that of the non-adaptive M-QAM for given SNR and BER_{tg} .

We compare several adaptive transmission techniques in Fig. 5. Perfect CSI is assumed. Continuous rate and power adaptation [1] is included in the comparison. Note that the method places no restrictions on the constellation size, which makes it impractical. We also found that the fixed-rate truncated channel inversion [1] based on M-QAM has similar

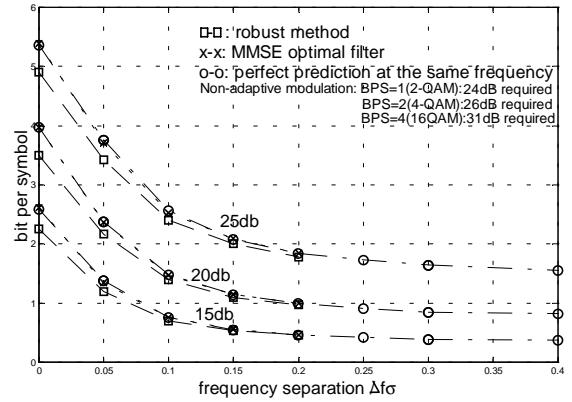


Fig.6. BPS vs. normalized frequency separation for different prediction techniques. $f_{\text{dm}} = 100\text{Hz}$. Prediction range 2ms. Target BER = 10^{-3} .

performance to the discrete power discrete rate method, while it is also non-feasible in practice. We also plot the Shannon capacity of the fading channel [1]. We observe that our continuous power control policy achieves about 3dB gain relative to the fixed power discrete rate adaptive modulation, and the discrete rate discrete power method has power loss of less than 2dB relative to the continuous power discrete rate transmission scheme.

Finally, we illustrate the performance of continuous power discrete rate adaptive M-QAM aided by channel prediction in Fig. 6. The symbol rate is 25ksymbol/s, and the modulation-switching rate is set to the symbol rate. Interpolation is utilized to predict the channel coefficients at the symbol rate. In Fig. 6 we plot bits per symbol vs. normalized frequency separation $\Delta f\sigma$ for the ideal (non-adaptive) MMSE filter (5-6) and the robust method using LMS (8-9) algorithm with step size 0.005 and estimated $\rho = 0.97$ and $\lambda = 0.995$. We also plot the BPS of the ideal robust method assuming that prediction is perfect at frequency f^1 . (It has almost the same performance as the optimal MMSE algorithm.) The figure shows that the robust method achieves near-optimal performance, while maintaining the ability to adapt transmission parameters to the time-variant channel conditions.

Fig. 6 also shows that adaptive modulation is primarily beneficial when normalized frequency separation $\Delta f\sigma$ does not significantly exceed 0.1. (For example, for $\Delta f\sigma = 0.1$, about 17dB is required to obtain 1 BPS for adaptive M-QAM as opposed to 24dB for non-adaptive transmission (2-QAM or BPSK.)) As frequency separation increases, the BPS approaches that of non-adaptive transmission. Hence the frequency separation and the multipath delay (or the coherence bandwidth) are the factors that determine the performance of the proposed adaptive modulation method.

The typical values of σ are on the order of microseconds in outdoor mobile radio channel [14]. Suppose $\Delta f\sigma = 0.1$ and $\sigma = 1\mu\text{sec}$. Then the frequency separation $\Delta f = 100\text{KHz}$. This means that two channels can be separated by 100KHz

and still benefit from the proposed adaptive transmission method. If $\sigma = 10\mu$ sec, smaller $\Delta f \leq 10\text{KHz}$ will result in good spectral efficiency when adaptive transmission is used.

4. CONCLUSION

We presented a novel adaptive modulation method that uses predicted CSI of a different carrier. The statistical model of the prediction accuracy factor was created and system performance was evaluated for various frequency separation values. We showed that increased frequency separation and multipath delay limit the performance of this system. The results can be applied in OFDM systems or in correlated uplink and downlink channels to reduce feedback and overhead requirements.

REFERENCES

- [1] A.J. Goldsmith, and S.G. Chua, "Variable-Rate Variable-Power MQAM for Fading Channels," *IEEE Trans. Commun.*, vol. 45, No 10, Oct 1997, pp.1218-1230.
- [2] A.J. Goldsmith, and S.G. Chua, "Adaptive Coded Modulation for Fading Channels," *IEEE Trans. Commun.*, vol. 46, No. 5, May 1998, pp.595-601.
- [3] T. Ue, S. Sampei, N. Morinaga, and K. Hamaguchi, "Symbol Rate and Modulation Level-Controlled Adaptive Modulation/TDMA/TDD System for High-Bit-Rate Wireless Data Transmission," *IEEE Trans. Veh. Technol.*, vol. 47, No. 4, Nov. 1998, pp.1134-1147.
- [4] D.L. Goeckel, "Adaptive Coding for Fading Channels Using Outdated Channel Estimates," *Proceedings of VTC*, May 1998, pp.1925-1929.
- [5] K. Miya, O. Kato, K. Homma, T. Kitade, M. Hayashi, and T. Ue, "Wideband CDMA Systems in TDD-mode Operation for IMT-2000," *IEICE Trans. Commun.*, vol. E81-B, July 1998, pp.1317-1326.
- [6] T. Eyceoz, A. Duel-Hallen, and H. Hallen, "Deterministic Channel Modeling and Long Range Prediction of Fast Fading Mobile Radio Channels," *IEEE Commun. Lett.*, vol. 2, No. 9, Sept. 1998, pp.254-256.
- [7] T. Eyceoz, S. Hu, and A. Duel-Hallen, "Performance Analysis of Long Range Prediction for Fast Fading Channels," *Proc. of 33rd Annual Conf. on Inform. Sciences and Systems CISS'99*, vol. II, March 1999, pp.656-661.
- [8] T. Eyceoz, S. Hu, and, A. Duel-Hallen, "Adaptive Prediction, Tracking and Power Adjustment for Frequency Non-Selective Fast Fading Channels," *Proc. of the Commun. Theory Mini-Conference, ICC'99*, June 1999, pp.1-5.
- [9] S. Hu, A. Duel-Hallen, H. Hallen, "Long Range Prediction Makes Adaptive Modulation Feasible for Realistic Mobile Radio Channels," *Proc. of 34rd Annual Conf. on Inform. Sciences and Systems CISS'2000*, vol. I, March 2000, pp.WP4-7~WP4-13.
- [10] A. Duel-Hallen, S. Hu and, H. Hallen, "Long Range Prediction of Fading Signals: Enabling Adaptive Transmission for Mobile Radio Channels," *IEEE Signal Processing Mag.*, vol. 17, No. 3, pp.62-75, May 2000.
- [11] S. Hu, A. Duel-Hallen, H. Hallen, "Adaptive Modulation Using Long Range Prediction for Fast Flat Fading Channels," *Proc. of IEEE Int. Symp. On Inform. Theory, ISIT'2000*, June 2000, p.159.
- [12] W. C. Jakes, *Microwave Mobile Communications*. Wiley, New York, 1974.
- [13] J. G. Proakis, *Digital Communications*. Third Edition, McGraw-Hill, 1995.
- [14] T. S. Rappaport, *Wireless Communications: Principles and Practice*. Prentice-Hall, 1996.
- [15] H. Hallen, S. Hu, M. Lei and, A. Duel-Hallen, "A Physical Model for Wireless Channels to Understand and Test Long Range Prediction of Flat Fading," *Proc. of WIRELESS 2001*, Calgary, Canada, July 2001, pp.99-107.